Pergamon

Int. J. Heat Mass Transfer. Vol. 39, No. 11, pp. 2303–2310, 1996
Copyright © 1996 Elsevier Science Ltd
Printed in Great Britain. All rights reserved
0017–9310/96 $15.00+0.00

0017–9310(95)00317–7

Variation of temperature and velocity fluctuations in turbulent thermal convection over horizontal surfaces

RONALD J. ADRIAN
Department of Theoretical and Applied Mechanics, University of Illinois, Urbana, IL 61801, U.S.A.

(*Received* 16 *January* 1995 *and in final form* 9 *August* 1995)

Abstract—The variations of root-mean-square (r.m.s.) temperature and velocity in turbulent thermal convection above a heated, horizontal surface are analyzed by extending the arguments of Castaing *et al.* ([1]: *J. Fluid Mech.* **204,** 1–30 (1989)) which lead to the two-sevenths power law for heat transfer. Asymptotic matching of properties scaled on Deardoff's convection scales with those scaled on Castaing *et al.*'s lambda-layer show that the r.m.s. temperature decays as $z^{-1/2}$ and the r.m.s. vertical velocity increases as log z. These results are supported by data from Rayleigh convection and unsteady convection, both penetrative and non-penetrative. Copyright © 1996 Elsevier Science Ltd.

INTRODUCTION

Turbulent thermal convection in fluid layers lying over heated horizontal surfaces contains warm, buoyant fluid elements which lose temperature excess by heat transfer to the surroundings and gain vertical velocity by buoyant acceleration as they rise upwards. The converse process takes place when negatively buoyant fluid descends from a cooled horizontal surface. Since buoyant fluid creates a large proportion of the turbulent fluctuations in the velocity and temperature, the intensities of fluctuation, as measured by root-mean-square (r.m.s.) values, change systematically with height. This variation of the intensities is necessary empirical input to various models of turbulent dispersion and mixing, and it characterizes the turbulent flow field in a fundamental way.

Figure 1 indicates schematically the profiles of the mean temperature, T, the total heat flux

$$Q(z) = \langle w\theta \rangle - \kappa \frac{\mathrm{d}T}{\mathrm{d}z} \qquad (1)$$

the r.m.s. of the vertical velocity fluctuation $\sigma_w = \langle w^2 \rangle^{1/2}$, and the r.m.s. of the turbulent temperature fluctuation θ, $\sigma_\theta = \langle \theta^2 \rangle^{1/2}$. Here brackets denote ensemble averaging, z is the vertical coordinate, g is the acceleration of gravity, and κ is the thermal diffusivity. The figure shows two configurations: Rayleigh convection between a hot lower surface and a cold upper surface, Fig. 1(a), and unsteady convection between a hot lower surface and an insulated upper surface, Fig. 1(b). The layer depth is denoted by z^*, and the layer is assumed to be wide compared to its depth. In Rayleigh convection, the total heat flux is constant, $Q = Q_o$, whereas in unsteady convection the total heat flux decreases linearly from the value Q_0 applied to the lower surface to zero at the upper surface (assuming it is perfectly insulating). Unsteady convection over a hot surface is just the mirror image of convection between a cooled upper surface and an insulating lower surface. To a first approximation Rayleigh convection can be modeled as a combination of the two in which hot buoyant fluid ascends from the lower surface and cold buoyant fluid descends from the top surface. In this simple model the two linear heat flux profiles sum to produce the constant heat flux that must occur in Rayleigh convection.

While the r.m.s. fluctuations of Rayleigh convection and unsteady convection above heated surfaces differ qualitatively in the top half of each layer, they are each similar in the bottom half. In general, the r.m.s. velocity increases from zero at the surface to a maximum close to the middle of the layer. The r.m.s. temperature, on the other hand, rapidly increases to a maximum, then decays to a minimum near the center of the layer in Rayleigh convection, or near the top in unsteady convection. An important difference between the unsteady case and Rayleigh convection is that the volume integrated buoyant production of turbulent kinetic energy is lower in the unsteady case. Offutt [2] has shown that using the volume averaged heat flux in the definition of velocity and temperature scales accounts for this difference and collapses the various profiles of r.m.s. quantities approximately onto one curve when properly scaled. Thus, the phenomena occurring in the lower half of each type of convection are substantially similar.

Priestley's [3, 4] similarity laws for the variation of r.m.s. vertical velocity, and r.m.s. temperature describe their behavior in a layer that is far enough above the heated surface to be unaffected by surface layer phenomena such as heat conduction, and far

NOMENCLATURE

A	empirical constant
B	empirical constant
b	empirical constant
F	dimensionless function
f	dimensionless function
g	gravitational acceleration [m s^{-2}]
N_0	empirical constant
Nu	Nusselt number
Pr	Prandtl number
Q	kinematic heat flux [°C m s^{-1}]
Q_0	kinematic heat flux at lower surface [°C m s^{-1}]
Ra	Rayleigh number
Ra_f	flux Rayleigh number
T	mean temperature
w	vertical velocity [m s^{-1}]
w_h	lambda layer velocity scale [m s^{-1}]
z	vertical distance above lower surface [m]
z_*	vertical depth of fluid layer [m].

Greek symbols

β	thermal coefficient of expansion [°C^{-1}]
ΔT	temperature difference [°C]
Δ_m	lambda layer temperature scale [°C]
κ	thermal diffusivity [m^2 s^{-1}]
λ	thickness of the lambda-layer [m]
ν	kinematic viscosity [m^2 s^{-1}]
σ	root mean square
θ	temperature fluctuation [°C].

Subscripts

w	vertical velocity
0	conduction layer scaling
*	convection layer scaling
θ	temperature.

enough below the top of the layer to be unaffected by the depth of the layer, z_*. Consequently, they pertain to a layer somewhat above the location of the peak of the r.m.s. temperature and somewhat below the center of the layer, indicated schematically in Fig. 1. The laws state that the r.m.s. of w is proportional to $z^{1/3}$ and r.m.s. of temperature is proportional to $z^{-1/3}$. These results are derived from a dimensional analysis in which the only relevant length scale is assumed to be the height above the surface, z. A related law for the mean temperature gradient, $\mathrm{d}T/\mathrm{d}z \sim z^{-4/3}$ was also derived by Priestley [3, 4] using dimensional analysis,

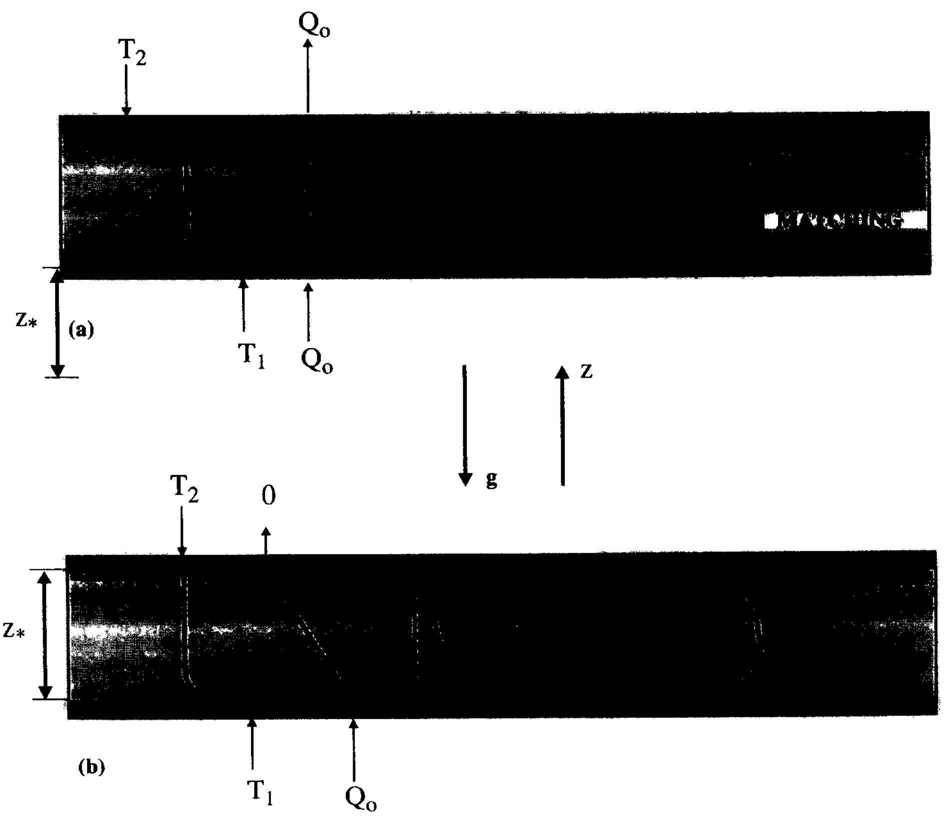

Fig. 1. Types of convection and definition of scales. (a) Rayleigh, (b) unsteady non-penetrative.

and earlier by Prandtl [5] who used a mixing length formulation based on the height above the surface. It is common to refer to these collectively as the Priestley similarity laws.

The outer region of the thermal convection layer scales very well with Deardorff's [6] convection scales:

$$\text{length scale} = z_* \quad w_* = (\beta g Q_0 z_*)^{1/3} \quad \theta_* = Q_0/w_*. \tag{2a–c}$$

In these equations β is the coefficient of thermal expansion. These scales have been shown to correlate data ranging from laboratory scale experiments up to atmospheric scale experiments [7], spanning over eighteen orders of magnitude in the Rayleigh number. They are derived under the assumption of a balance between buoyant and inertial term, and negligible conductive heat flux.

The correct scales for the region close to the heated surface are less well established. Townsend [8] showed good correlation of data in convection over a single heated surface by using the molecular scales

$$z_0 = \kappa/w_0 \quad w_0 = (\beta g Q_0 \kappa)^{1/4} \quad \theta_0 = Q_0/w_0. \tag{3a–c}$$

Here the assumption is that the conductive transfer of heat dominates, and that the layer is thin compared to z_*, so that z_* is not an important variable. With this scaling the momentum balance must be between the buoyancy and the viscous terms, with inertia being negligible, as it is implicit in (3a) that the Peclet number and hence the Reynolds number must be of order one for Prandtl number of order unity. Practically this means that the Reynolds number must be bounded by a constant as Rayleigh number becomes infinite. A similar set of variables, modified by a weak dependence on Prandtl number has been shown to correlate the profiles of mean temperature very well for water and air data [9].

The Priestley similarity laws can be derived by asymptotically matching scaling laws based on Deardorff's convection scales with scaling laws based on Townsend's molecular transfer scales [7, 9, 10]. This process leads to power laws in a manner analogous to Millikan's [11] development of the famous logarithmic law in forced convection (see also [12]).

The classical result of scaling arguments for heat transfer in Rayleigh convection is the one-third law for the Nusselt number–Rayleigh number relation:

$$Nu = N_0 Ra^{1/3} \tag{4}$$

where

$$Nu = Q_0 z_*/\kappa\,\Delta T \tag{5}$$

$$Ra = \beta g\,\Delta T z_*^3/\kappa\nu. \tag{6}$$

Here, N_0 is a constant, ν is the kinematic viscosity and ΔT is the total temperature drop. In these arguments all of the temperature drop is supposed to occur in the inner layers, and to be controlled by the scales of that layer only. The one-third exponent on the Rayleigh number implies that the Nusselt number is independent of the total layer depth, z_*. The one-third law for heat transfer is also frequently associated with Priestley's laws for the variation of the mean temperature gradient, $dT/dz \sim z^{4/3}$ [12].

In the unstable planetary boundary layer, where the Reynolds number is very high and the lowest layer is one of turbulent forced convection, there is support for Priestley similarity of the r.m.s. velocity and temperature [13, 14], although the scatter of the data is large. However in laboratory convection experiments, the evidence is less convincing [7]. Moreover, the exponent of the heat transfer relation is very clearly not equal to one-third [1, 15, 16] with most results in the range 0.278–0.30.

λ-LAYER SCALING

The observations of Castaing *et al.* [1] of Rayleigh convection over a six decade wide range of Rayleigh numbers provide convincing evidence that the Nusselt number varies in proportion to the Rayleigh number raised to the two-sevenths power in this range. Their experimental results give

$$Nu = 0.23 Ra^{0.282} \tag{7}$$

where the uncertainty of the exponent is 0.282 ± 0.006. They offer two alternative derivations of this result, each based on simple arguments that involve two layers: a core layer which is inertial and buoyant and a 'mixed' layer which is a viscous, inertial and buoyant layer, in which molecular heat conduction and turbulent heat transfer are comparable. In the alternative derivations the core layers are the same, but different relationships are developed for the mixed layer.

It can be shown that the analysis of the core layer given by Castaing *et al.* [1] is equivalent to the derivation of the convection layer scales given by Deardorff [6]. Thus, the core layer is the same as the high Reynolds number convection layer discussed in earlier work [7], and as noted above, there is very good evidence for Deardorff scaling of this layer, extending up to atmospheric Reynolds numbers. The novel part of the analysis of Castaing *et al.* [1] postulates a wall layer of length scale λ that lies below the convection layer. It can be shown that their first analysis of this layer is equivalent to postulating that it scales with

$$\lambda \equiv z_*/Nu = \kappa\,\Delta T/Q_0 \quad w_h = \beta g\,\Delta T \lambda^2/\nu$$
$$\text{temperature scale} = \Delta T. \tag{8a–c}$$

The length scale λ in (8a) was originally proposed by Kraichnan [17] as a measure of the depth of the wall layer at which half of the heat flux is convective and half is conductive. It is, therefore a mixed region of turbulent motion and molecular diffusion. (Since ΔT is the total temperature drop across both wall layers in Rayleigh convection, it would be more appropriate to use $\Delta T/2$ for each wall layer. For the purpose of scaling arguments Castaing, *et al.* ignore the factor of two, and we shall do likewise.) Castaing *et al.* [1] found the velocity scale in equation (8b) by balancing the fluctuating vertical buoyant force with the viscous stress, under the assumption that fluid elements in the wall layer have temperature excess of order ΔT and length scale for viscous shear of order λ. It is implicit that the stresses acting on the fluid are laminar viscous stresses, which limits the domain of validity of the analysis to a low Reynolds number layer close to the wall. Thus, the arguments should not be applied to convection in the atmosphere where the layer lying beneath the convective layer is highly turbulent forced convection.

We shall refer to the layer defined by (8a) as the λ-*layer*.

Equations (2) and (8) do not complete the problem without one further relationship. The critical assumption used to effect closure in the first model proposed by Castaing *et al.* [1] is that the velocity scale of the λ-layer is equal to the velocity scale of the convective layer:

$$w_h = w_*. \tag{9}$$

With this relation, equations (2b), (8a), (8b) and (9) lead immediately to

$$Nu = N_0 Pr^{1/7} Ra^{2/7} \tag{10}$$

for Rayleigh convection. A similar relation can be found for unsteady convection with properly defined Rayleigh and Nusselt numbers. In either case the relationship

$$\frac{\Delta T}{\theta_*} = Pr^{1/2}\left(\frac{\lambda}{z}\right)^{-1/2} \tag{11}$$

follows from equations (2), (8) and (9). The model comprised of (2a–c), (8a–c) and (9) will be called the λ-I model.

A second theory, which will be called the λ-II model, was also developed on the basis of Deardorff convection scaling in the core layer, equations (2a) and (2b), Kraichnan's length scale relation, equation (8a), and a new temperature scale given by

$$\Delta_m = \frac{\kappa\nu}{\beta g\lambda^3}. \tag{12}$$

This scale represents the temperature of the λ-layer after the thermals in the layer have mixed by turbulent motion. A detailed physical argument leading to (12) is given in Castaing *et al.* [1], but it can also be found by dimensional analysis under the assumption that neither z_* nor Q_0 affect the temperature scale of the λ-layer. The critical assumption in the λ-II model which effects closure is that the temperature scale of the λ-layer is equal to the temperature scale of the core convection layer,

$$\Delta_m = \theta_*. \tag{13}$$

By themselves, equations (2a), (2b), (8a) and (12) plus (13) are sufficient to predict the two-sevenths relationship in (10). Castaing *et al.* [1] view this as a more reasonable assumption than that of equal velocity scales used in the λ-I model. While it is not necessary to define a velocity scale in the λ-II model in order to arrive at the two-sevenths law, the scale implied by Castaing *et al.* [1] is just (8b). Interestingly, the equations (2a), (2b), (8a), (12) and (13) also imply that w_h is just equal to w_*, as in (9). Hence the λ-II model can be summarized as a statement of dimensional analysis that the λ, w_*, Δ_m scales pertain in the λ-layer, and that $\Delta_m = \theta_*$.

PROFILES OF THE R.M.S. QUANTITIES

λ-I Model

As previously noted, it is well established that in the outer, convection layer the profile of σ_w is a universal function of z/z_*, independent of the Reynolds number or the Rayleigh number for all sufficiently large values. Let us denote this function by F_w:

$$\sigma_w/w_* = F_w(z/z_*). \tag{14}$$

Likewise, the success of the λ-layer scaling in predicting the two-sevenths law suggests that σ_w ought to be a universal function in the λ-layer also:

$$\sigma_w/w_h = f_w(z/\lambda). \tag{15}$$

Following Millikan [11] the functions can be found by requiring that their derivative with respect to z match for all Rayleigh numbers (or, equivalently all values of z_*/λ, since this ratio depends on the Rayleigh number). Hence,

$$d\sigma_w/dz = (w_*/z_*)F'_w(z/z_*) = (w_h/\lambda)f'_w(z/\lambda). \tag{16}$$

Setting $w_h = w_*$ and multiplying by z gives

$$(z/z_*)F'_w(z/z_*) = (z/\lambda)f'_w(z/\lambda) \tag{17a}$$

$$= A_w \tag{17b}$$

where (17b) follows because each side, being functions of different arguments can only be equal for all Rayleigh numbers if they are constants. The integral of (17) gives

$$\sigma_w/w_* = A_w \ln(z/\lambda) + b_w \quad \sigma_w/w_* = A_w \ln(z/z_*) + B_w \tag{18a,b}$$

where b_w and B_w are independent of z, but may depend on Pr.

Note that the logarithmic variation results fundamentally from the fact that the velocity scale is the same in both layers, cf. equation (9). In Millikan's treatment of pipe and channel flow the logarithmic law for the mean velocity profile comes about because the friction velocity scales both the outer layer and the inner layer. In the present context given the scales identified for the λ-I layer and the convection layer, the equality of the velocity scales simultaneously implies the two-sevenths law and the logarithmic law. However, the logarithmic variation would result from any scaling argument in which the velocity scales were set equal, independent of whether or not the Nusselt number–Rayleigh number relationship obeyed the two-sevenths power law.

The profile of σ_θ can also be obtained by asymptotically matching dimensionless scaling laws of the λ-layer and the convection layer:

$$\sigma_\theta/\Delta T = f_\theta(z/\lambda) \quad \sigma_\theta/\theta_* = F_\theta(z/z_*). \quad (19a,b)$$

Equating the gradient leads to

$$d\sigma_\theta/dz = (\theta_*/z_*)F'_\theta(z/z_*) = (\Delta T/\lambda)f'_\theta(z/\lambda) \quad (20)$$

which becomes

$$F'_\theta = Pr^{1/2}(z_*/\lambda)^{3/2}f'_\theta \quad (21)$$

after using (11). Multiplying by $(z/z_*)^{3/2}$ yields an equation that contains a function of (z/z_*) on the left and (z/λ) on the right

$$(z/z_*)^{3/2}F'_\theta = Pr^{1/2}(z/\lambda)^{3/2}f'_\theta \quad (22)$$

and to match asymptotically each term must be a constant which we shall call $-A_\theta$. Integrating equation (22) then gives

$$\sigma_\theta/\Delta T = A_\theta Pr^{-1/2}(z/\lambda)^{-1/2} + b_\theta$$

$$\sigma_\theta/\theta_* = A_\theta(z/z_*)^{-1/2} + B_\theta. \quad (23)$$

λ-II Model

In the second model of Castaing *et al.* [1] equality of the temperature scales and the velocity scales in the λ-II layer and the convection layer imply that σ_θ and σ_w each obey logarithmic laws similar in form to (18). Thus, the λ-I and λ-II models predict the same variation for σ_w, but distinctly different variation for σ_θ.

Experimental profiles

The foregoing scale arguments and asymptotic matching analyses are identical for unsteady convection and Rayleigh convection, aside from the fact that the values of the various constants may differ due to the differences between the heat flux profiles. For this reason, results for unsteady convection will be presented separately from those for Rayleigh convection.

The r.m.s. vertical velocity shown in Fig. 2 is taken from unsteady, non-penetrative convection experiments in water [7] and the large eddy simulations of air [18]. The data from [7] cover a range of heat fluxes and layer depths. The flux Rayleigh number defined by

$$Ra_f = \beta g Q_0 z^4{}_*/\kappa^2\nu \quad (24)$$

affords an unambiguous basis for comparing the unsteady convection and Rayleigh convection. For the data from ref. [7] in Fig. 2 $8.48\times10^9 < Ra_f$, 2.64×10^{11}. The flux Rayleigh number of the LES result, being a simulation of the atmosphere, is much larger. Agreement between the data and the logarithmic curve (solid line) is within the statistical sampling error of the measurements. The logarithmic fit spans a range from $z/z_* = 0.004$ to about 0.1, approximately a one-and-one-half decade range.

Profiles of the r.m.s. velocity found in the Rayleigh convection simulations of Moeng and Rotunno [20] at $Ra = 3.8\times10^5$ and Kerr [21] at 2×10^7 are shown in Fig. 3. Both are highly resolved direct numerical simulations that give r.m.s. vertical velocities at the centerline which agree closely with the experimental measurements of Deardorff and Willis [19] which are also shown. The latter data were taken at $Ra = 10^7$, corresponding to $Ra = 1.7\times10^8$. Kerr's [21] results corresponded to $Ra_f = 3.4\times10^8$. Filled and unfilled symbols represent data from the top and bottom halves of the Rayleigh convection layer, respectively. While there is some difference in slope, all of the data

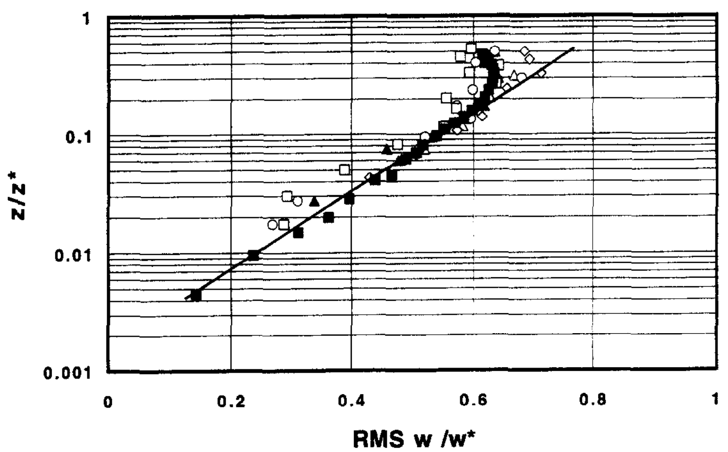

Fig. 2. Root-mean-square of the vertical velocity fluctuation in unsteady non-penetrative convection. Filled squares: Schmidt and Schumann [18]; other symbols: Adrian *et al.* [7]. The solid line is a logarithmic curve.

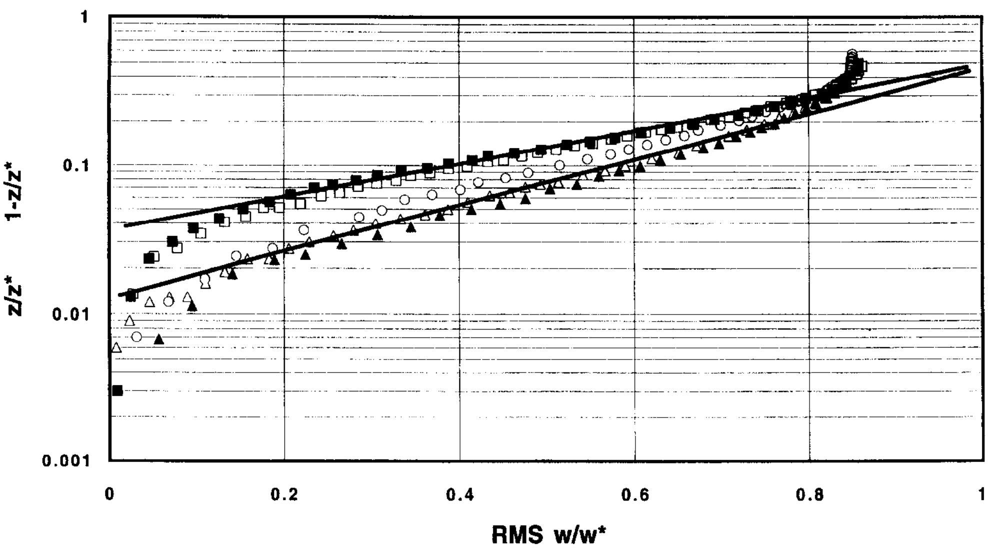

Fig. 3. Root-mean-square of the vertical velocity fluctuation in Rayleigh convection. ○ : Deardorff and Willis [19]; ■, □ : Moeng and Rotunno [20]; ▲, △ : Kerr [21]. The solid line is a logarithmic curve.

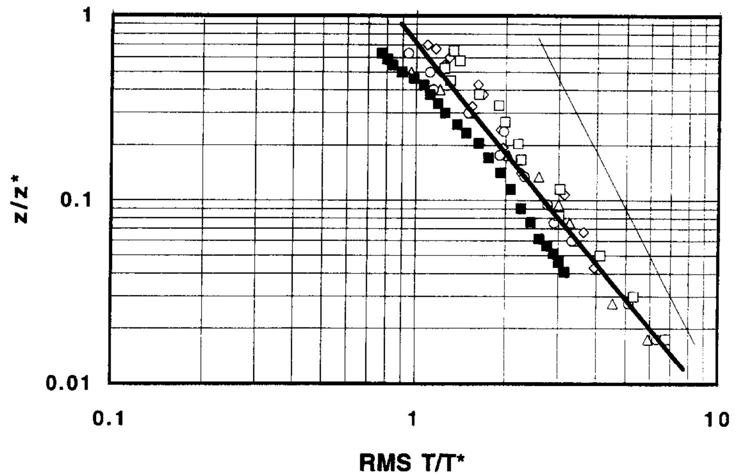

Fig. 4. Root-mean-square of the temperature fluctuation in unsteady non-penetrative convection. Filled squares: Schmidt and Schumann [18]; other symbols: Adrian *et al.* [7]. The heavy solid line is a $z^{-1/2}$ slope, and the light solid line is a $z^{-1/3}$ slope.

can be fitted to a logarithmic curve over a range of heights between $0.02 < z/z^* < 0.2$, similar to the range found in Fig. 2, and consistent with the range expected for the overlap between the λ-layer and the convection layer. The results in Figs. 2 and 3 support the logarithmic law stated in equation (18), and offer indirect support for the equality of the velocity scales of the λ-layer and the convection layer, equation (9). They do not, however discriminate between the λ-I and the λ-II models, since both models imply a logarithmic law.

Profiles of the r.m.s. temperature fluctuation are plotted in Fig. 4 using unsteady convection data from the same sources as in Fig. 2. Unsteady convection offers a better test of the r.m.s. temperature profile than Rayleigh convection because σ_θ varies over a greater range. In particular it decays to a smaller value far above the lower plate. The experimental data all scale well with the convection temperature scale, and generally follow a $z^{-1/2}$ power law (solid line). The LES data of ref. [18] lie below the best fit to the experimental data, but also generally follow the $z^{-1/2}$ slope. The $z^{-1/2}$ law is a much better fit to the data than the $z^{-1/3}$ law predicted by Priestley similarity, and it is a better fit to the experimental data than the logarithmic variation predicted by the λ-II model, cf. Fig. 5. However, the LES data in Fig. 5 fit the logarithmic variation as well as they fit the $z^{-1/2}$ profile.

Other experimental data offer less clear support for the new laws. Measurements of σ_w by Garon and Goldstein [22] agree better with the $z^{1/3}$ law than with the logarithmic law, but they are even fundamentally at odds with most data in that they do not scale well with Deardorff's convection velocity. Atmospheric results are generally thought to agree with the Priestley laws, but they are scattered enough to make agreement

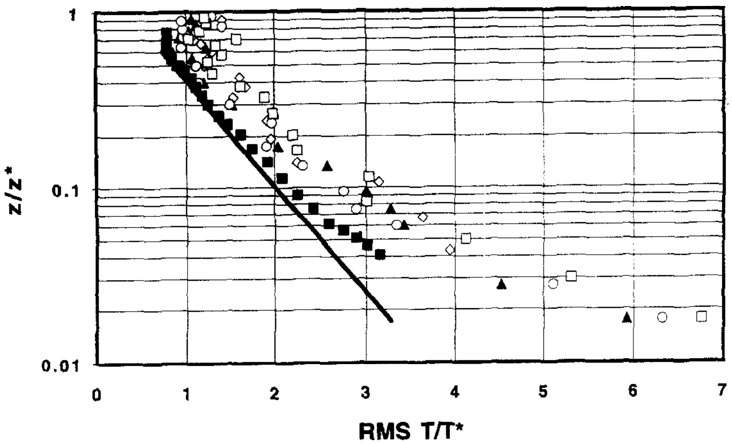

Fig. 5. Root-mean-square of the temperature fluctuation in unsteady non-penetrative convection. Symbols as in Fig. 4. The solid line is a logarithmic curve.

with the present results also possible. For example, Businger *et al.* [23] report that the mean temperature gradient varies as $dT/dz \sim z^{-3/2}$, consistent with the variation of the r.m.s. temperature derived here. However, the present matching assumes a viscous layer which surely does not exist in the atmospheric case, unless one invokes an analogy with small scale eddy viscosity. Croft [24] on the other hand also reports $dT/dz \sim z^{-3/2}$ in a laboratory experiment. Clearly, further work is needed to establish the limits of validity of any of the power laws.

Previously it was shown that asymptotically matching a layer that scales with Deardorff's convection layer variable to a layer that scales with Townsend's [8] wall layer variables leads to Priestley's laws for σ_w and σ_θ [7]. Further, Townsend's variables seem to give good correlation of the velocity and temperature statistics in the wall layer. How then is it that λ-layer scaling gives a better description? The answer to this question lies in the very small differences between Townsend's scales and those of the λ-layer. It is straightforward to show that

$$\frac{\Delta T}{\theta_0} = \frac{\lambda}{z_0} = N_0^{-3/2} Pr^{1/4} Ra^{-1/28} \tag{25}$$

and hence that the difference between the two scalings would not be revealed by direct examination unless the Rayleigh number were varied over very many decades. This range of Rayleigh numbers was not achieved until the experiment of Castaing *et al.* [1].

SUMMARY AND CONCLUSIONS

In turbulent thermal convection above wide horizontal surfaces the fluid mechanics in the layer close to the heated surface involves a balance between viscous diffusion, inertia and buoyancy, and far above the surface the flow is a balance of inertia and buoyancy. Classical analysis of the layer between the two regions implies that the r.m.s. of the temperature and velocity vary as $z^{-1/3}$ and $z^{1/3}$, respectively. These are the well-known similarity laws of Priestley [3, 4]. It has been shown that analysis consistent with the two-sevenths power law for the Nusselt number–Rayleigh number relation, equation (7), implies a new set of laws in which the r.m.s. vertical velocity varies as the logarithm of height, equation (18), and the r.m.s. temperature fluctuation varies as $z^{-1/2}$, equation (23). Results from Rayleigh convection and unsteady convection agree better with these laws than with the Priestley laws, presenting a consistent picture whose essential elements are the λ-I layer scaling in equation (8) and equality of the λ-layer velocity scale and Deardorff's convection scale.

Although the analyses presented here are based on matching arguments applied in the limit of infinite Rayleigh number, it is unlikely that they actually hold for very large Rayleigh numbers because the λ-layer scaling fundamentally implies a Reynolds number, $w_* \lambda / \nu$ that grows without bound as Ra increases, and this must ultimately violate the assumption of a viscous–inertial–buoyant balance. The Reynolds number is easily shown to be given by

$$w_* \lambda / \nu = N_0^{-2} Pr^{-2/3} Ra^{1/7}. \tag{26}$$

If one estimates a transition from laminar to turbulent flow for Reynolds number between 100 and 1000, the corresponding transition Rayleigh number is of order 10^{14}–10^{21}. Even the lower bound exceeds the Rayleigh number attained in the experiments of Castaing *et al.* [1], indicating that behavior consistent with a viscous λ-layer may not be observed at higher values of Ra. This may explain why Priestley similarity laws are observed in the atmosphere, where the Reynolds numbers are such that the layer adjacent to the ground is fully turbulent.

Acknowledgement—Research supported by National Science Foundation grant ATM 89-20605.

REFERENCES

1. B. Castaing, G. Gunaratne, F. Heslot, L. Kadanoff, A. Libchaber, S. Thomae, X.-Z. Wu, S. Zaleski and G.

Zanetti, Scaling of hard thermal turbulence in Rayleigh–Bénard convection, *J. Fluid Mech.* **204**, 1–30 (1989).
2. P. W. Offutt, Thermal convection, Ph.D. Thesis, University of Illinois, Urbana, IL (1995).
3. C. H. B. Priestley, Free and forced convection in the atmosphere near the ground, *Q. J. R. Met. Soc.* **81**, 139–143 (1955).
4. C. H. B. Priestley, *Turbulent Transport in the Lower Atmosphere*. University of Chicago Press, Chicago (1959).
5. L. Prandtl, Meterologische Anwendungen der Stromungslehre, *Beitr. Phys. Atmos.* **19**, 188–202 (1932).
6. J. W. Deardorff, Convective temperature and velocity scales for the unstable planetary layer and for Rayleigh convection, *J. Atmos. Sci.* **27**, 1211–1213 (1970).
7. R. J. Adrian, R. T. D. S. Ferreira and T. Boberg, Turbulent thermal convection in wide horizontal fluid layers, *Exp. Fluids* **4**, 121–141 (1986).
8. A. A. Townsend, Temperature fluctuations over a heated horizontal surface, *J. Fluid Mech.* **5**, 209–241 (1959).
9. M. K. Chung, H. C. Yun and R. J. Adrian, Scale analysis and wall layer model for the temperature profile in a turbulent thermal convection, *Int. J. Heat Mass Transfer* **35**, 43–51 (1992).
10. T. Boberg, An experimental study of unsteady free convection from a heated horizontal plate, M.S. Thesis, University of Illinois, Urbana, IL (1977).
11. C. B. Millikan, A critical discussion of turbulent flow in channels and circular tubes, *Proceedings of the Fifth International Congress in Applied Mechanics*, pp. 386–392 (1937).
12. R. R. Long, Relation between Nusselt number and Rayleigh number in turbulent thermal convection, *J. Fluid Mech.* **73**, 445–451 (1976).
13. J. C. Kaimal, R. A. Eversole, D. H. Lenschow, B. B. Stankov, P. H. Kahn and J. A. Businger, Spectral characteristics of the convective boundary layer over uneven terrain, *J. Atmos. Sci.* **39**, 1098–1114 (1982).
14. Z. Sjorban, *Structure of the Atmospheric Boundary Layer*. Prentice Hall, Englewood Cliffs, NJ (1989).
15. R. J. Goldstein and T. Y. Chu, Thermal convection in a horizontal layer of air, *Prog. Heat Mass Transfer* **2**, 55–75 (1969).
16. T. Y. Chu and R. J. Goldstein, Turbulent convection in a horizontal layer of water, *J. Fluid Mech.* **60**, 141–159 (1973).
17. R. H. Kraichnan, Turbulent thermal convection at arbitrary Prandtl number, *Phys. Fluids* **5**, 1374–1389 (1962).
18. H. Schmidt and U. Schumann, Coherent structure of the convective boundary layer derived from large-eddy simulations, *J. Fluid Mech.* **200**, 511–562 (1989).
19. J. W. Deardorff and G. E. Willis, Investigation of turbulent thermal convection between horizontal plates, *J. Fluid Mech.* **28**, 675–704 (1967).
20. C. H. Moeng and R. Rotunno, Vertical velocity skewness in the buoyancy driven boundary layer, *J. Atmos. Sci.* **47**, 1149–1162 (1990).
21. R. M. Kerr, Rayleigh number scaling in numerical convection, private communication (1994).
22. A. M. Garon and R. J. Goldstein, Velocity and heat transfer measurements in thermal convection, *Phys. Fluids* **16**, 1818–1825 (1973).
23. J. A. Businger, J. C. Wyngaard, Y. Izumi and E. F. Bradley, Flux–profile relationships in the atmospheric surface layer, *J. Atmos. Sci.* **28**, 181–189 (1971).
24. J. F. Croft, The convection regime and temperature distribution above a heated horizontal surface. *Q. J. R. Met. Soc.* **91**, 151–157 (1958).